Arabidopsis HMA2, a Divalent Heavy Metal-Transporting P_{IB}-Type ATPase, Is Involved in Cytoplasmic Zn^{2+} Homeostasis[1]

Elif Eren and José M. Argüello*

Department of Chemistry and Biochemistry, Worcester Polytechnic Institute, Worcester, Massachusetts 01609

P_{IB}-type ATPases transport heavy metal ions (Cu^+, Cu^{2+}, Zn^{2+}, Cd^{2+}, Co^{2+}, etc.) across biological membranes. Several members of this subfamily are present in plants. Higher plants are the only eukaryotes where putative Zn^{2+}-ATPases have been identified. We have cloned *HMA2*, a P_{IB}-ATPase present in Arabidopsis (*Arabidopsis thaliana*), and functionally characterized this enzyme after heterologous expression in yeast (*Saccharomyces cerevisiae*). HMA2 is a Zn^{2+}-dependent ATPase that is also activated by Cd^{2+} and, to a lesser extent, by other divalent heavy metals (Pb^{2+}, Ni^{2+}, Cu^{2+}, and Co^{2+}). The enzyme forms an acid-stable phosphorylated intermediate and is inhibited by vanadate. HMA2 interacts with Zn^{2+} and Cd^{2+} with high affinity (Zn^{2+} $K_{1/2} = 0.11 \pm 0.03$ μM and Cd^{2+} $K_{1/2} = 0.031 \pm 0.007$ μM). However, its activity is dependent on millimolar concentrations of Cys in the assay media. Zn^{2+} transport determinations indicate that the enzyme drives the outward transport of metals from the cell cytoplasm. Analysis of *HMA2* mRNA suggests that the enzyme is present in all plant organs and transcript levels do not change in plants exposed to various metals. Removal of *HMA2* full-length transcript results in Zn^{2+} accumulation in plant tissues. *hma2* mutant plants also accumulate Cd^{2+} when exposed to this metal. These results suggest that HMA2 is responsible for Zn^{2+} efflux from the cells and therefore is required for maintaining low cytoplasmic Zn^{2+} levels and normal Zn^{2+} homeostasis.

Zn^{2+} plays a critical role in plants as an essential component of key enzymes (Cu-Zn superoxide dismutase, alcohol dehydrogenase, RNA polymerase, etc.) and DNA-binding proteins (Marschner, 1995; Guerinot and Eide, 1999). Zn^{2+} deficiency leads to a reduction of internodal growth with a consequent rosette-like development and also produces an impaired response to oxidative stress, likely due to a reduction in superoxide dismutase levels (Hacisalihoglu et al., 2003). Thus, Zn^{2+} deficiency is a significant agricultural problem, particularly in cereals, limiting crop production and quality (Guerinot and Eide, 1999; Hacisalihoglu et al., 2003). Zn^{2+} toxicity induces chlorosis in young leaves, probably via competition with Fe^{2+} and Mg^{2+} (Woolhouse, 1983; Marschner, 1995).

Zn^{2+}, as other metal micronutrients, is essential for normal physiology; however, plants must also protect themselves from hazards associated with chemical modifications that these and nonessential metals (Cd^{2+}, Pb^{2+}, etc.) can drive (Woolhouse, 1983; Clemens, 2001; Fraústro da Silva and Williams, 2001; Hall, 2002). Consequently, plants and other organisms have developed molecular chaperones, chelators, and specific transmembrane transporters to (1) absorb and distribute metal micronutrients throughout the entire organism and (2) prevent high cytoplasmic concentrations of free heavy metals ions (Fox and Guerinot, 1998; Rauser, 1999; Guerinot, 2000; Williams et al., 2000; Clemens, 2001; Cobbett and Goldsbrough, 2002; Hall, 2002). These processes require the metal to be transported through permeability barriers and compartments delimited by lipid membranes. Several types of heavy metal transmembrane transporters have been identified in plants (Rea, 1999; Guerinot, 2000; Maser et al., 2001; Baxter et al., 2003). Since metal ions must be transported against electrochemical gradients at some point during plant distribution, metal pumps involved in contragradient transport should play key roles in metal homeostasis. The presence of plant genes encoding proteins that specifically perform this function (mainly P_{IB}-ATPases) is known and their potential importance has been repeatedly noted (Williams et al., 2000; Clemens, 2001; Hall, 2002).

P_{IB}-ATPases, a subfamily of P-type ATPases, transport heavy metals (Cu^+, Ag^+, Cu^{2+}, Zn^{2+}, Cd^{2+}, Pb^{2+}, and Co^{2+}) across biological membranes (Lutsenko and Kaplan, 1995; Axelsen and Palmgren, 1998; Argüello, 2003). Initial reports named these proteins CPx-ATPases (Solioz and Vulpe, 1996). They confer metal tolerance to microorganisms (Solioz and Vulpe, 1996; Rensing et al., 1999) and are essential for the absorption, distribution, and bioaccumulation of metal micronutrients by higher organisms (Bull and Cox, 1994;

[1] This work was supported by the U.S. Department of Agriculture (grant no. 2001–35106–10736) and by the National Science Foundation (grant no. MCM–0235165).

* Corresponding author; e-mail arguello@wpi.edu; fax 508–831–5933.

Article, publication date, and citation information can be found at www.plantphysiol.org/cgi/doi/10.1104/pp.104.046292.

Solioz and Vulpe, 1996). Most P_{IB}-ATPases appear to have eight transmembrane segments (Melchers et al., 1996; Tsai et al., 2002; Argüello, 2003). Like all other P-type ATPases, they have a large ATP-binding cytoplasmic loop between their sixth (H6) and seventh (H7) transmembrane segments. Within this loop, the Asp in the signature sequence DKTGT is phosphorylated during the catalytic cycle (Lutsenko and Kaplan, 1995; Axelsen and Palmgren, 1998). Two other structural characteristics are usually considered to differentiate P_{IB}-ATPases: the signature sequence (CPC, CPH, CPS, SPC, and TPC) in H6, and the frequently present metal-binding domains in the cytoplasmic N-terminal region (Bull and Cox, 1994; Solioz and Vulpe, 1996; Rensing et al., 1999; Argüello, 2003; Lutsenko and Petris, 2003). P_{IB}-ATPases appear to have a catalytic mechanism similar to that of well-characterized enzymes in the subgroup P_{II} of the P-type ATPase family (plant H-ATPase, Na,K-ATPase, sarcoplasmic reticulum Ca-ATPase, etc.). Our group and others have established the formation of the phosphorylated intermediate and basic transport properties for some bacterial, archaeal, and mammalian P_{IB}-ATPases (Tsai et al., 1992; Tsai and Linet, 1993; Solioz and Odermatt, 1995; Rensing et al., 1998a, 1998b; Voskoboinik et al., 1998, 1999; La Fontaine et al., 1999; Okkeri and Haltia, 1999; Sharma et al., 2000; Fan and Rosen, 2002; Mandal et al., 2002; Mana-Capelli et al., 2003; Mandal and Argüello, 2003). Both in vivo and in vitro metal transport studies have shown that P_{IB}-ATPases drive the export of ions from the cell cytoplasm (Tsai et al., 1992; Tsai and Linet, 1993; Rensing et al., 1998a, 1998b; Voskoboinik et al., 1998, 1999; Fan and Rosen, 2002; Mandal et al., 2002; Mana-Capelli et al., 2003).

The P_{IB}-ATPase subfamily includes proteins with different metal specificities (Cu^+-ATPases, Cu^{2+}-ATPases, Zn^{2+}-ATPases, Co^{2+}-ATPases, etc.) and a particular protein often can transport various metals (Rensing et al., 1999; Argüello, 2003). Functional assays have shown that Ag^+ can also activate Cu^+-ATPases (Solioz and Odermatt, 1995; Fan and Rosen, 2002; Mandal et al., 2002), Zn^{2+}-ATPases can use Cd^{2+} and Pb^{2+} as substrates (Tsai et al., 1992; Tsai and Linet, 1993; Okkeri and Haltia, 1999; Sharma et al., 2000), and Cu^{2+}-ATPases can also be partially activated by Ag^+ and Cu^+ (Mana-Capelli et al., 2003). Although it has been proposed that the Cys-containing sequences in H6 participate in metal binding and transport (Bull and Cox, 1994; Lutsenko and Kaplan, 1995; Solioz and Vulpe, 1996; Axelsen and Palmgren, 1998; Rensing et al., 1999; Mandal and Argüello, 2003), the relationship between ion specificity and the various conserved sequences in H6 (CPC, CPH, SPC, TPC, or CPS) is not fully understood. However, true signature sequences in H6, H7, and H8 have been identified and they appear to be associated with five subtypes of P_{IB}-ATPases, each with singular metal selectivity characteristics (Argüello, 2003). These conserved amino acids are likely located close to each other, participating in metal coordination and consequently determining the enzyme specificity.

Arabidopsis (*Arabidopsis thaliana*) has eight genes encoding P_{IB}-ATPases (heavy metal ATPases [HMA]). (We have chosen to use the nomenclature recently proposed by Baxter et al. [2003] and adopted in the PlantsT database [http://plantst.sdsc.edu]. Consequently, the proteins previously named PAA1, RAN1, and HMA6 are referred to here as HMA6, HMA7, and HMA8, respectively.) A search through other plant genomes (see http://www.tigr.org or http://plantst.sdsc.edu) reveals the presence of many putative orthologs (Axelsen and Palmgren, 2001; Baxter et al., 2003). Since other eukaryotes appear to have only two Cu^+-ATPase isoforms, the presence of multiple, distinct P_{IB}-ATPase isoforms seems unique to plants (Argüello, 2003). The analysis of conserved residues in their transmembrane segments suggest that three are Zn^{2+}-ATPases (HMA2, 3, and 4) and four are Cu^+-ATPases (HMA5, 6, 7, and 8; Argüello, 2003). The remaining protein, HMA1, has different conserved amino acids in the transmembrane region. The only HMA1 homolog that has been studied is CoaT from *Synechocystis* PCC6803, which appears to confer Co^{2+} tolerance to this organism (Rutherford et al., 1999). Additionally, the primary sequences of plant P_{IB}-ATPases suggest the presence of various putative metal-binding domains in their cytoplasmic loops. These are likely to play important regulatory roles, such as those observed in similar domains of other P_{IB}-ATPases (Voskoboinik et al., 2001; Mana-Capelli et al., 2003; Mandal and Argüello, 2003).

Several of the plant P_{IB}-ATPases, HMA2, HMA3, and HMA4 (putative Zn^{2+}-ATPases), and HMA6 and HMA7 (putative Cu^+-ATPases originally named PAA1 and RAN1), have been the subject of characterization studies (Hirayama et al., 1999; Woeste and Kieber, 2000; Mills et al., 2003; Shikanai et al., 2003; Gravot et al., 2004; Hussain et al., 2004). *ran1-1* and *ran1-2*, two *HMA7* mutants, are partially functional and can replace Ccc2 (a Cu^+-ATPase) in Δ*ccc2* yeast (*Saccaromyces cerevisiae*; Hirayama et al., 1999). *ran1-1* plants present ethylene phenotypes in response to trans-cyclooctene (ethylene antagonist; Hirayama et al., 1999). As Cu is part of the ethylene receptor, a decrease in the number of functional receptors was proposed. A third mutant, *ran1-3*, produces a truncated mRNA and shows constitutive activation of ethylene response pathways and a rosette lethal phenotype. Transgenic *35S::RAN1* plants show constitutive expression of ethylene response due to cosuppression of *RAN1* (Woeste and Kieber, 2000). The requirement to produce functional ethylene receptors suggests a post-Golgi location for HMA7. Arabidopsis mutants that are defective in the *HMA6* (*PAA1*) gene show a high-chlorophyll fluorescence phenotype due to a decrease in holoplastocyanin and a consequent reduction in photosynthetic electron transport (Shikanai et al., 2003). Addition of Cu^{2+} suppresses this phenotype. These studies suggest that HMA6 is responsible for Cu^+ transport into chloroplasts.

Putative Zn^{2+}-ATPases present in Arabidopsis are particularly interesting because, as mentioned above, plants are the only eukaryotes where these proteins are present. Initial studies of HMA4 have shown that this enzyme is able to confer cell resistance to high Cd^{2+} or Zn^{2+} when expressed in yeast or *Escherichia coli*, respectively (Mills et al., 2003). In Arabidopsis, high levels of *HMA4* transcripts are observed mainly in roots and are increased upon plant exposure to high Zn^{2+} levels (Mills et al., 2003). Arabidopsis HMA3 confers Cd^{2+} and Pb^{2+} tolerance to Δ*ycf1* yeast cells and a green fluorescent protein-tagged HMA3 appears located at the yeast vacuole (Gravot et al., 2004). *HMA3* mRNA is detected mainly in roots and its level is not affected in response to exposure to Cd^{2+} or high Zn^{2+}. A recent report has shown that, while no morphological alterations were observed in *hma2* or *hma4* Arabidopsis mutants, an *hma2 hma4* double mutant shows visible morphological alterations and male sterility (Hussain et al., 2004). These phenotypes can be compensated by increasing Zn^{2+} levels in the growth medium. Interestingly, decreased levels of Zn were detected in shoots of the *hma2 hma4* mutant and *hma4* single mutant, while increased levels of this metal were detected in roots of the double mutant. In addition, Hussain et al. showed that HMA2 and HMA4 promoters drive the expression of a reporter gene predominantly in vascular tissues and that HMA2 is localized at the plasma membrane in Arabidopsis cells (Hussain et al., 2004). In summary, previous reports have shown the likely role of these proteins in Zn^{2+} homeostasis and Cd^{2+}/Pb^{2+} tolerance; however, the molecular properties that determine their physiological functions have not been established.

Toward understanding the physiological roles of Zn-ATPases in plants, we initiated enzymatic and metal transport studies of Arabidopsis HMA2. This article describes the molecular characteristics of this metal-transporting ATPase and its consequent role in metal homeostasis. Ion selectivity, activity rate, direction of transport, catalytic phosphorylation, and interaction with Cys (a P_{IB}-type ATPase activator) and vanadate (a classical inhibitor of P-type ATPases) were measured. The presence of *HMA2* mRNA in different plant organs and its variation upon plant exposure to various metals was determined together with the effect of *HMA2* knockout on Zn^{2+} homeostasis. The results obtained indicate that HMA2 drives the efflux of Zn^{2+} from plant cells. Thus, HMA2 appears responsible for maintaining low cellular Zn^{2+} levels.

RESULTS

The *HMA2* cDNA was amplified by reverse transcription (RT)-PCR. The obtained sequence was identical to that expected from genome sequencing, confirming the intron/exon predictions. The 951-amino acid-long encoded protein shows characteristic features of P_{IB}-ATPases (Fig. 1). Signature sequences corresponding to Zn^{2+}-ATPases are found in H6, H7, and H8, and analysis with topology prediction software suggests that it has eight transmembrane segments (Argüello, 2003). HMA2 contains a relatively short N-terminal end with significant homology to the heavy metal-associated domain (PF00403; Bateman et al., 2004). However, it is unlikely that this would have a regulatory role as the typical N-terminal metal-binding domains observed in Cu^{+}-ATPases, since a Cys critical for metal binding is not present in HMA2 (CysXXCys → Cys-17CysThrSer-20; Voskoboinik et al., 1999, 2001; Lutsenko and Petris, 2003). HMA2 has a long C-terminal end (258 amino acids) characterized by the presence of several short sequences that might be involved in heavy metal binding: six CysCys pairs, five HisXHis repeats, and two repeats of the sequence GXDSGCCGXKSQQPHQHEXQ (starting at Gly-794 and Gly-824). Supporting the participation of these putative metal-binding sequences in common regulatory mechanisms, several of them can be found in the C-terminal ends of both HMA2 and HMA4 (S^{797}GCCG; S^{827}GCCG; S^{760}SDHSHSGCC; C^{930}CRSYAKESCSHDHHHTRAH; positions correspond to the HMA2 sequence).

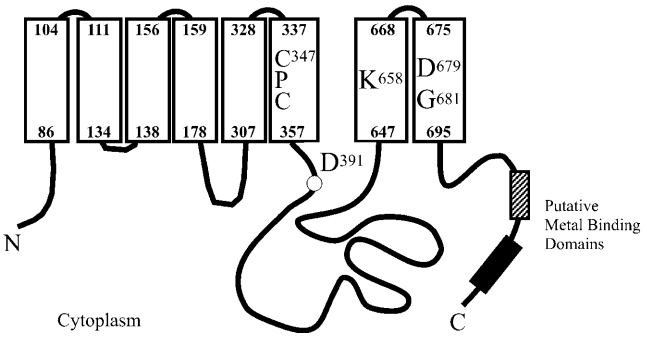

Figure 1. Structural features of HMA2. Transmembrane segments are represented by white rectangles. Numbers in bold indicate the position of transmembrane segments within the HMA2 sequence. Asp-391 is phosphorylated during the catalytic cycle and conserved in all P-type ATPases. Cys-347ProCys, Lys-658, Asp-679, and Gly-681 are conserved in all Zn^{2+}-ATPases and are likely determinants of the enzyme specificity. Striped and black blocks represent putative metal-binding domains.

Functional Characterization of HMA2

A central point for understanding the role of HMA2 is to elucidate its metal specificity and enzymatic properties. We chose to functionally characterize this enzyme after expressing it in yeast under the control of the *GAL* promoter. Figure 2 shows the expression of HMA2 in a membrane vesicle preparation from transformed yeast. HMA2 expression was routinely detected by immunostaining blots with anti-His_6 antibodies. Control experiments showed no differences in metal-dependent ATPase activity or metal affinity among membrane preparations of the His_6-tagged

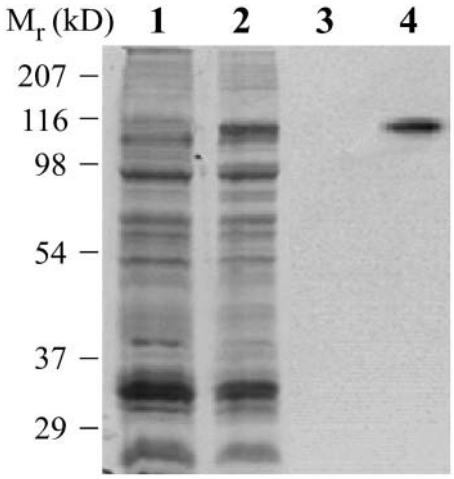

Figure 2. Expression of Arabidopsis HMA2 in yeast. Membrane preparations from untransformed yeast (lanes 1 and 3) and Gal-induced yeast transformed with HMA2-pYES2/CT (lanes 2 and 4). Lanes 1 and 2, Coomassie Brilliant Blue-stained gel; lanes 3 and 4, blot immunostained with anti-His_6 rabbit polyclonal IgG (Santa Cruz Biotechnology, Santa Cruz, CA) and donkey anti-rabbit IgG-horseradish peroxidase-linked monoclonal antibody (Santa Cruz Biotechnology).

HMA2 and those of protein lacking the tag (data not shown). It should be noted that, in the following ATPase and phosphorylation experiments, saponin was included in the assay media to permeabilize sealed vesicles present in the membrane preparations.

ATPase activity determinations indicate that HMA2 is a Zn^{2+}-ATPase as expected from its signature sequence in the transmembrane region (Fig. 3). HMA2 is also activated by Cd^{2+} (97%) and other divalent metals (Ni^{2+}, Co^{2+}, Cu^{2+}, and Pb^{2+}), although to a lesser extent (34%–52%). Even Cu^{+} elicits a measurable activity. Confirming that the measured activity was associated with HMA2, no measurable heavy metal-dependent ATPase activity was detected in membranes obtained from yeast transformed with empty pYES2/CT vector. The activity observed in the presence of Ni^{2+}, Cu^{2+}, Co^{2+}, and Pb^{2+} is not surprising since another biochemically characterized Zn^{2+}-ATPase, *E. coli* ZntA, is also partially activated by these metals, although to different extents (Okkeri and Haltia, 1999; Sharma et al., 2000). The kinetics parameters describing the metal interaction with HMA2 were evaluated by measuring the dependence of ATPase activity on metal concentration (Fig. 4). These determinations show that HMA2 is activated by Zn^{2+} and Cd^{2+} with surprisingly high affinity (Zn^{2+} $K_{1/2}$ = 0.11 ± 0.03 μM and Cd^{2+} $K_{1/2}$ = 0.031 ± 0.007 μM). In the analysis of the specificity and function of metal transporters, the apparent absence of free heavy metals in living systems should be considered. Both cytoplasmic [Cu] and [Zn] appear to be in the picomolar range under physiological conditions (Rae et al., 1999; Outten and O'Halloran, 2001). In this direction, the dependence of P_{IB}-ATPase activity on the presence of millimolar Cys in the assay media has been proposed to be an indication of the interaction of the metal complex with these enzymes (Sharma et al., 2000; Mandal et al., 2002). Figure 5 shows that HMA2 activity was also dependent on the presence of millimolar Cys in the media, suggesting that plant P_{IB}-ATPases also appear to require the delivery of complexed metals for activity.

The unifying functional characteristic of all P-type ATPases is the formation of a phosphorylated intermediate in the presence of ATP-Mg and the outwardly transported substrate (i.e. the ion that is transported out of the cytoplasm into an organelle or the extracellular compartment; Pedersen and Carafoli, 1987). Phosphorylation of HMA2 was performed at 0°C in the presence of micromolar amounts of ATP and 20% dimethyl sulfoxide, conditions that minimize enzyme turnover. Preliminary experiments in which the samples were resolved in acid gels and their radioactivity visualized using a phosphoimager indicated that, under the experimental conditions, a single band corresponding to HMA2 was phosphorylated in the presence of Zn^{2+} (Fig. 6A). Protein phosphorylation was not observed in membranes from yeast transformed with the empty pYES2/CT vector. Similar results were obtained with all tested metals. For simplicity, in subsequent experiments HMA2 phosphorylation was directly quantified counting radioactive emission (Fig. 6B). Levels of phosphoenzyme in the presence of various metals roughly follow the activation pattern observed in the ATPase determina-

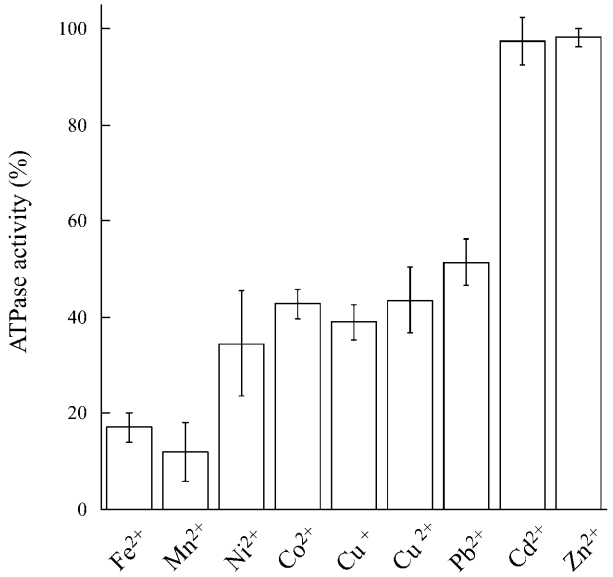

Figure 3. Activation of HMA2 ATPase by metals. HMA2 ATPase activity was determined as indicated in "Materials and Methods." Final concentration of each tested metal ion was 1 μM, which is a saturating concentration for all of them. A total of 2.5 mM DTT were included in Cu^{+}-containing assay mixture. Bars indicate activity in the presence of each metal as percentage of maximum activity. One-hundred percent = 1.8 to 2.5 μmol mg^{-1} h^{-1}. Values are the mean ± SE (n = 4).

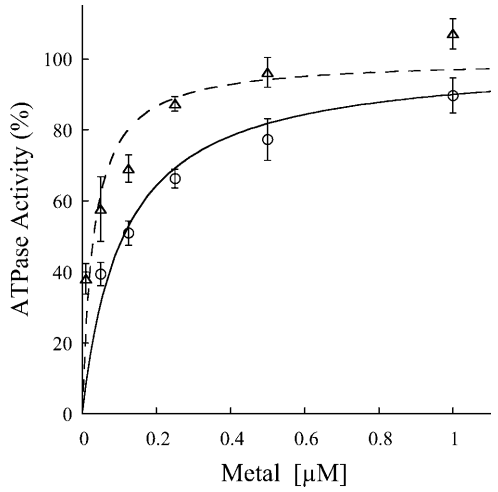

Figure 4. Zn^{2+} and Cd^{2+} dependence of HMA2 ATPase activity. The ATPase activity was measured in the presence of different concentrations of Zn^{2+} (○) or Cd^{2+} (△) ions. Data were fitted using the following parameters: Zn^{2+} $K_{1/2}$ = 0.11 μM, V_{max} = 100%; Cd^{2+} $K_{1/2}$ = 0.031 μM, V_{max} = 100%. One-hundred percent = 2 to 2.5 μmol mg^{-1} h^{-1}. Values are the mean ± SE (n = 4).

tions (Fig. 3). The small variations are not surprising since these determinations are not equally related to the metal interaction with the enzyme (Mandal et al., 2002; Hou and Mitra, 2003). Figure 6B also shows the inhibition of phosphorylation by vanadate, a well-known feature of P-type ATPases; however, in the case of HMA2, vanadate inhibits its ATPase activity with a slightly high IC_{50} = 0.15 ± 0.05 mM (not shown). The quantitative determination of phosphoenzyme levels allows the calculation of HMA2 turnover number. Assuming that under the maximum phosphorylation conditions (in the presence of Cd^{2+}) most of the enzyme is arrested in the E1P-E2P conformations, and taking into account the activity of the particular HMA2 preparations used in the phosphorylation assays (2 μmol mg^{-1} h^{-1}), a turnover of 143 min^{-1} was calculated. This value is similar to those observed in other P_{IB}-ATPases (Mandal et al., 2002).

Although the phosphorylation determinations suggest that HMA2 transports metals out of the cytoplasm, it is pertinent to directly demonstrate the direction of metal transport by this enzyme. To this end, the vesicular nature of the yeast membrane preparation can be exploited. Although this preparation might contain broken vesicles, only sealed inside-out vesicles would be able to perform ATP-dependent metal transport. Similar yeast membrane preparations have been used to measure Cu^{+} transport by heterologously expressed human ATP7A (Voskoboinik et al., 2001). The Zn^{2+} level outside the vesicles was monitored using the membrane-impermeable, fluorescent Zn indicator FluoZin-1 (Gee et al., 2002). Figure 7 shows the ATP-dependent Zn^{2+} uptake into HMA2-containing vesicles. In these experiments, as the metal is transported into the vesicles, the level of Zn-FluoZin-1 complex decreases and a consequent reduction of its fluorescence is detected. The observed decline in the uptake rate after 8 to 10 min is likely associated with enzyme inhibition by high intravesicular Zn^{2+}. Further evidence that the decrease in fluorescence is due to ATP-dependent Zn^{2+} transport by HMA2 is provided by the absence of Zn^{2+} uptake in the presence of 1.5 mM vanadate or ADP (replacing ATP in the assay medium). Similar lack of Zn^{2+} uptake was observed in experiments performed using membranes from yeast transformed with empty pYES2/CT vector. In summary, these results clearly indicate that HMA2 drives Zn^{2+} export from the cell cytoplasm.

Analysis of *HMA2* Transcript Levels

The role of *HMA2* in the Zn^{2+} homeostasis in plants is also determined by its location and regulation upon plant exposure to various conditions. In a first approach to establish these characteristics, *HMA2* mRNA levels were measured in roots, leaves, stems, and flowers from 6-week-old plants and 10-d-old seedlings using semiquantitative RT-PCR. Figure 8A shows significant *HMA2* transcript levels in all tested organs. Although slightly higher levels were detected in roots (50% higher than in leaf), the similar distribution in all organs suggests the ubiquitous expression of this ATPase. Similar levels of *HMA2* mRNA were observed when seedlings were exposed to various metals (Fig. 8B), albeit up-regulation can be detected in the presence of Ag^{+} (53%) or Co^{2+} (66%). These findings can be compared with similar studies of two other Arabidopsis Zn^{2+}-ATPases. Different from *HMA2*, *HMA3* and *HMA4* mRNAs are more abundant in roots, and HMA4 transcription appears to be up-regulated in the presence of Zn^{2+} or Mn^{2+} and down-regulated in the presence of Cd^{2+} (Mills et al., 2003; Gravot et al., 2004). Thus, *HMA2*'s distinct transcript distribution

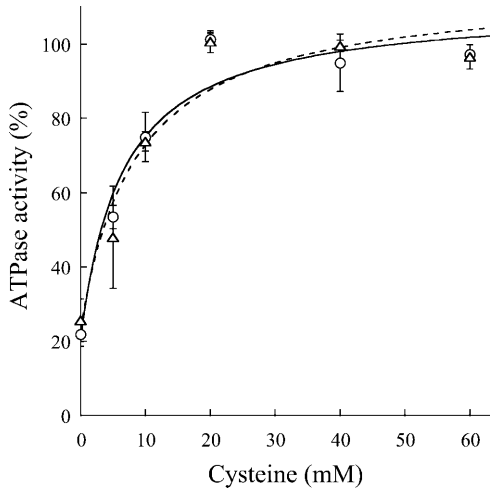

Figure 5. Cys dependence of HMA2 ATPase activity. The Zn^{2+} (○) and Cd^{2+} (△) dependent ATPase activities were determined as indicated in "Materials and Methods" in the presence of various Cys concentrations. No curve fitting was attempted. One-hundred percent = 2 to 2.5 μmol mg^{-1} h^{-1}. Values are the mean ± SE (n = 4).

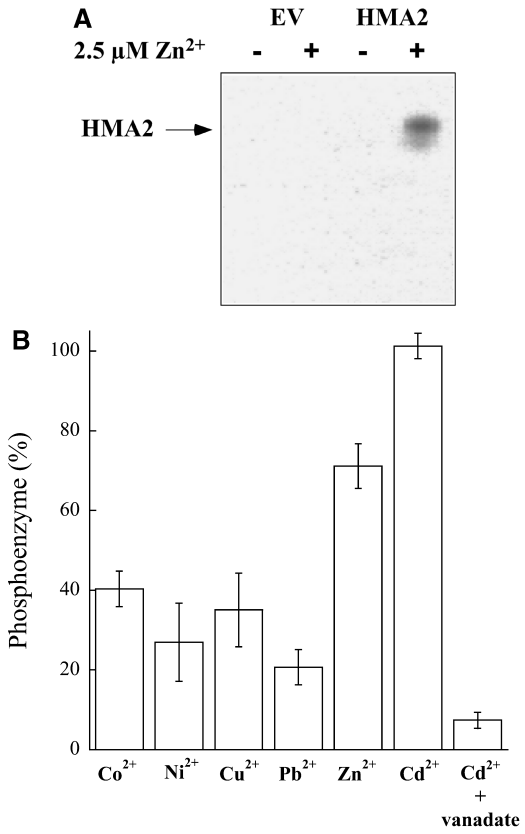

Figure 6. Metal-dependent phosphorylation of HMA2 by ATP. A, Membrane preparations from yeast-transformed empty vector (EV) and HMA2-expressing yeast (HMA2) were phosphorylated in the absence (−) or presence (+) of 2.5 μm Zn^{2+}, resolved by SDS-PAGE in an 8% acidic gel, and visualized in a phosphoimager. HMA2 protein is indicated. B, The metal-activated enzyme phosphorylation by ATP was measured as described in "Materials and Methods." One-hundred percent = 0.232 nmol mg^{-1}. Values are the mean ± SE (n = 4).

pattern and regulation of expression suggest a unique role for this gene.

Analysis of Zn^{2+} Homeostasis in *hma2* Mutant Plants

Homozygous plants for a T-DNA insert in the first intron of the *HMA2* gene were isolated by screening the Salk_034292 Arabidopsis line (Alonso et al., 2003; Fig. 9). In a recent report, Hussain et al. (2004) described the isolation of homozygous plants for this mutant line and named it *hma2-4*. By performing backcrosses to wild type, these investigators verified that *hma2-4* plants segregated for a single T-DNA insert. In our laboratory, we determined that full-length HMA2 transcripts were absent in these plants (Fig. 9, C and D). *hma2-4* plants grow at a normal rate with no observable distinctive morphological phenotypes (Fig. 9F). Although *hma2-4* seedling roots appear 10% to 20% shorter than those of wild type, no statistically significant difference in root length could be established (not shown). Exposure of *hma2-4* plants (in soil or in agar) to Cd^{2+} or high Zn^{2+} did not reveal any growth or morphological alteration. These observations were supported by similar findings in *hma2-5* plants. This T-DNA insertion mutant was isolated by Harper and collaborators. *hma2-5* plants also lack full-length *HMA2* transcripts (Fig. 9E).

In spite of the absence of macroscopic changes, large alterations in Zn^{2+} homeostasis were observed in *HMA2* knockout plants. Under normal growth conditions, mutant plants show a 65% increase in whole-plant Zn^{2+} levels (Fig. 10A). This imbalance is also observed when plants are exposed to high Zn^{2+} concentrations (50%–130% increase). Keeping in mind that HMA2 exports Zn^{2+} from the cell cytoplasm, these results are in agreement with the location of this pump in the cell plasma membrane (Hussain et al., 2004). To test in vivo the HMA2 capacity of transporting Cd^{2+}, the effect of exposing wild-type and mutant plants to this metal was analyzed. In preliminary control experiments, the absence of Cd^{2+} in plants drenched in water was confirmed. When exposed to Cd^{2+}, *hma2-5* and *hma2-4* plants accumulate higher amounts of this metal than wild-type plants (Fig. 10B). Cd^{2+} accumulation mimics the increase in Zn^{2+} levels in mutant plants and is in agreement with the metal specificity determined in biochemical assays. It was also observed that wild-type plants accumulated more Zn^{2+} when exposed to Cd^{2+} (Fig. 10A). This is likely associated with competition of both cations for cell efflux systems, HMA2 among others. The specific competition of Zn^{2+} and Cd^{2+} for HMA2 is clearer when Zn^{2+} levels in Cd^{2+}-exposed *hma2-5* and *hma2-4* plants are analyzed (Fig. 10A). In this case, a reduction (25%–30%) in the Zn^{2+} levels is observed. These results can be interpreted in terms of a parsimo-

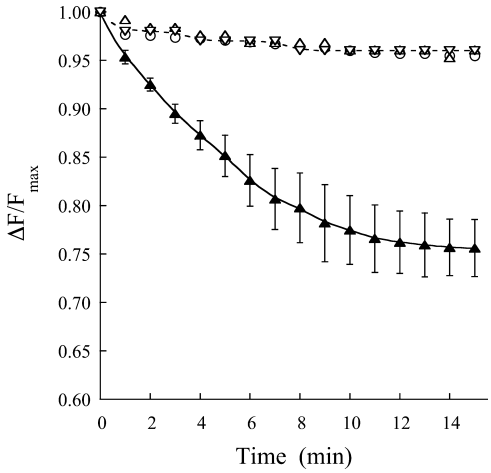

Figure 7. ATP-dependent Zn^{2+} transport by HMA2. Zn^{2+} uptake into empty vector-transformed yeast (△), HMA2-expressing yeast vesicles in the absence (▲) and presence of vanadate (○) or ADP (replacing ATP; ▽) was measured as indicated in "Materials and Methods." Results are shown as the relative change in fluorescence with respect to the maximum initial value. Values of uptake in the presence of ATP are the mean ± SE (n = 3).

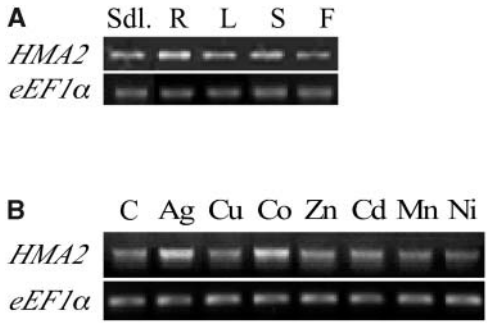

Figure 8. HMA2 transcript levels. RT-PCR (25 cycles) was used to amplify a 2,056-bp fragment of the *HMA2* mRNA. *eEF1α* amplification (20 cycles) was used as a control of total RNA levels. A, *HMA2* mRNA levels in various organs of 6-week-old plants. B, *HMA2* mRNA levels in 10-d-old seedlings grown in the presence of the indicated metal.

nious model where Zn^{2+} homeostasis is controlled by a cell influx component (transporter), an efflux system (a metal pump, HMA2), and a component that pumps the metal into an intracellular storage compartment. Thus, removal of the efflux system (in these experiments by HMA2 knockout) would lead to an increase in the Zn^{2+} level. Alternatively, even in the absence of efflux (HMA2 knockout), removal of transport into the intracellular compartment and/or influx system (in this experiment by high Cd^{2+} competition) would lead to a reduction in the Zn^{2+} total level. Finally, to verify that the observed effects are not the result of unspecific alterations in ionic homeostasis, Fe^{2+} levels were measured in wild-type, *hma2-5*, and *hma2-4* plants. No significant changes in the level of this ion were detected in the mutant plants compared to wild type.

DISCUSSION

Maintenance of Zn^{2+} homeostasis is required for normal plant physiology. This homeostasis is achieved by the specific and coordinated action of numerous secondary and primary transporters. Among these, Zn^{2+}-transporting P-type ATPases appear as likely key players considering their capacity for contraelectrochemical gradient transport and their unique presence in plants. Here we present experimental evidence for a determinant role of one of these enzymes, HMA2, in plant Zn^{2+} homeostasis.

HMA2 Biochemical Characteristics and Their Physiological Implications

HMA2 behaves as a classic P-type ATPase. It forms a phosphorylated intermediate in the presence of ATP and the outwardly transported metal and it is inhibited by vanadate. Similarly, HMA2 presents characteristics that are unique to P_{IB}-type ATPases. It is activated by several (similar) metals and requires Cys

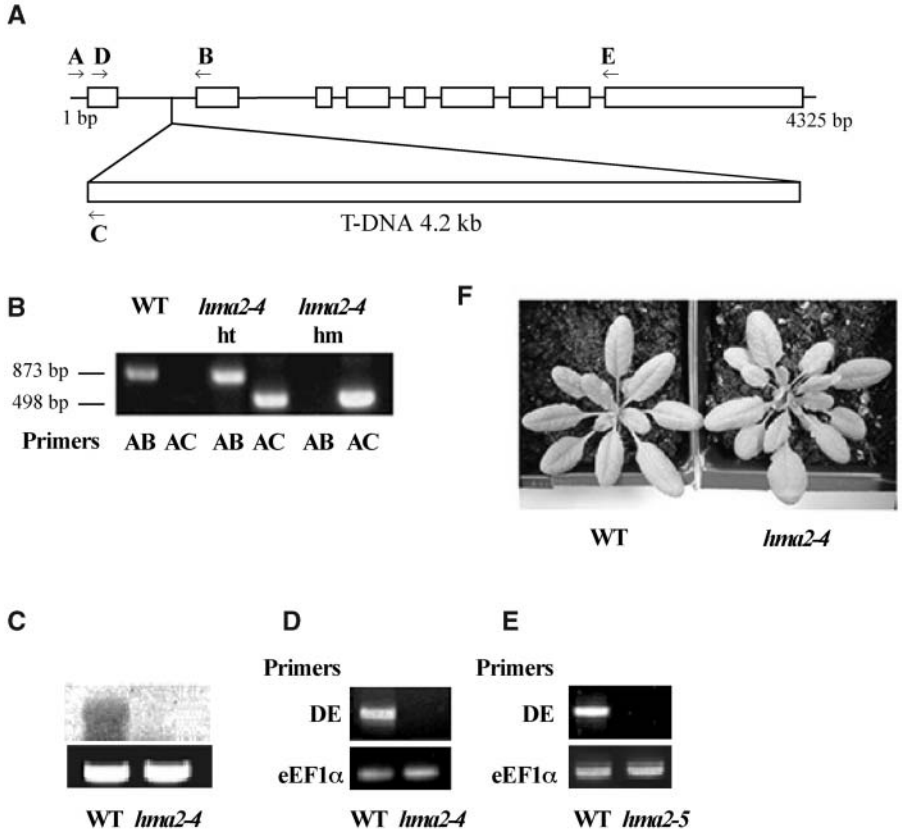

Figure 9. Isolation of *hma2-4* mutants. A, Schematic map of *HMA2* gene carrying a single copy of the T-DNA insert. Arrows indicate the annealing position of specific primers for the *HMA2* and left border of T-DNA insert. B, Screening of *hma2-4* mutants by PCR: DNA amplification for wild-type (WT), heterozygous *hma2-4* mutants (*hma2-4*, ht), and homozygous *hma2-4* mutants (*hma2-4*, hm) are shown. Bold letters indicate the primer pairs used for DNA amplification. C, Northern-blot analysis of *HMA2* mRNA levels in wild-type (WT) and homozygous *hma2-4* mutants (*hma2-4*). Equal amount of loading was verified by the staining of 18S rRNA with ethidium bromide (lower image). D, RT-PCR analysis of *HMA2* mRNA levels in wild-type (WT) and homozygous *hma2-4* mutants (*hma2-4*) using primers D and E. Equal amount of cDNA in each PCR tube was verified by amplification with *eEF1α* primers (lower image). E, RT-PCR analysis of *HMA2* mRNA levels in wild-type (WT) and homozygous *hma2-5* mutants (*hma2-5*) using primers D and E. Equal amount of cDNA in each PCR tube was verified by amplification with *eEF1α* primers (lower image). F, Wild-type and *hma2-4* plants grown in soil for 3 weeks.

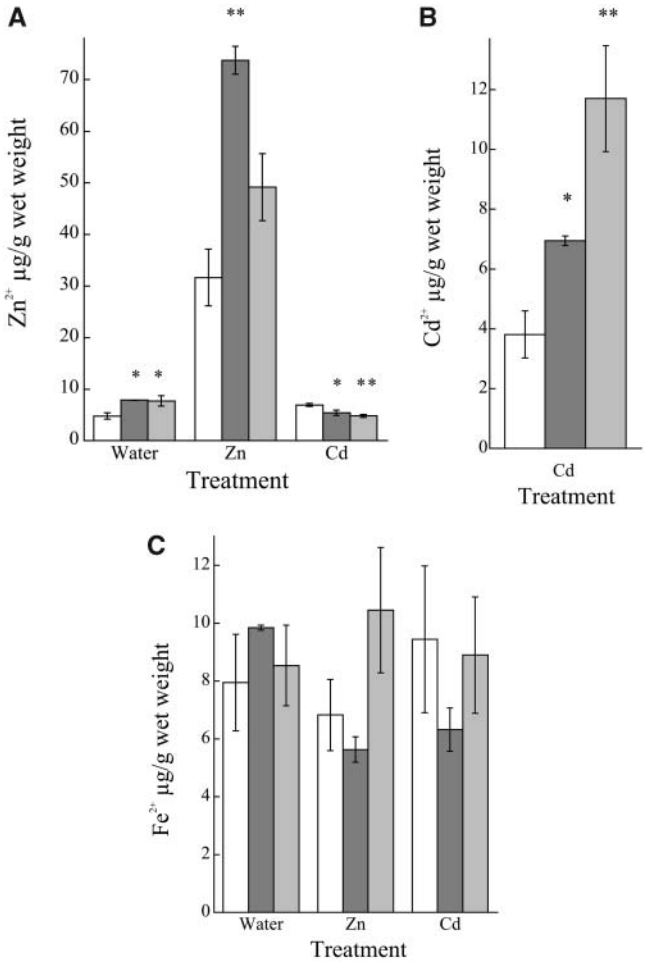

Figure 10. Zn^{2+}, Cd^{2+}, and Fe^{2+} levels in wild-type, *hma2-5*, and *hma2-4* plants. A, Zn^{2+} levels in wild-type (white bars), *hma2-5* (light gray bars), and *hma2-4* (dark gray bars) plants drenched in tap water (Water), 0.5 mM $ZnCl_2$ (Zn), or 0.125 mM $CdCl_2$ (Cd), as indicated in "Material and Methods." B, Cd^{2+} levels in wild-type, *hma2-5*, and *hma2-4* plants drenched in 0.125 mM $CdCl_2$. C, Fe^{2+} content of wild-type, *hma2-5*, and *hma2-4* plants treated as indicated above. Values are the mean ± SE ($n = 3$); tissue from three plants was pooled for each independent sample. Significant differences from the wild type as determined by Student's *t* test are indicated. $*P < 0.05$; $**P < 0.005$.

for full activity. Analysis of the enzyme metal dependence indicates that, in addition to Zn^{2+}, its likely physiological substrate, HMA2, is also activated by Cd^{2+}, Pb^{2+}, Ni^{2+}, Co^{2+}, and Cu^{2+}. This broad metal selectivity is common to other Zn-ATPases. For instance, HMA4 confers Zn^{2+} and Cd^{2+} resistance when expressed in *E. coli* and yeast, respectively (Mills et al., 2003), while HMA3-expressing *Δycf1* yeast cells present Cd^{2+} and Pb^{2+} tolerance (Gravot et al., 2004). A prokaryote HMA2 homolog, *E. coli* ZntA, is also activated by these divalent heavy metals (Okkeri and Haltia, 1999; Sharma et al., 2000). However, HMA2 and ZntA relative activities in the presence of various metals are different. ZntA appears activated by $Pb^{2+} \geq Zn^{2+} > Cd^{2+} > Ni^{2+} = Cu^{2+}$ (compare with Fig. 3). The multiselectivity of these enzymes is likely associated with the similar ionic radius, Lewis characteristics, and/or K_{eq} for the corresponding Cys complexes of these metals. On the other hand, the relative differences in activation patterns might be associated with small structural differences due to variations in nonmetal-coordinating amino acids located close to metal-binding sites (Argüello, 2003). These molecular characteristics have direct physiological effects since, in vivo, HMA2 does transport the nonphysiological substrates as evidenced by higher Cd^{2+} levels and the competition of Zn^{2+} and Cd^{2+} observed in *hma2-5* and *hma2-4* plants exposed to these metals.

HMA2 interacts with metals with particularly high affinity, approximately three orders of magnitude higher than those observed in ZntA (Sharma et al., 2000). This higher affinity for Zn^{2+} and other substrates might lead to lower cytoplasmic levels of these metals in plants. Although it is possible that this is based on a tighter metal coordination, it appears more likely that the high metal affinity is originated in the preference of HMA2 to remain in its E1 conformation. In this case, a higher apparent affinity for ligands (ATP and metals) that bind this form would be observed. Correspondingly, lower apparent affinities of those ligands binding E2 should be detected. This would explain the relatively high vanadate IC_{50} showed by HMA2. It is also interesting that HMA2 requires the presence of Cys in the assay medium for maximum activity as *E. coli* ZntA or *Archaeoglobus fulgidus* CopA (Cu^+-ATPase) do (Sharma et al., 2000; Mandal et al., 2002). Experiments with CopA suggest that Cys is not transported by these enzymes but is rather required for substrate delivery to the transmembrane transport sites (Y. Yang, A.K. Mandal, and J.M. Argüello, unpublished data). In plants, it might not be Cys but a similar complexing or chaperone molecule that delivers the metal to the enzyme. Soluble metal chaperones have been identified in plants (Himelblau et al., 1998).

Physiological Role of HMA2

The increase in Zn^{2+} and Cd^{2+} levels in *hma2* plants indicates that the enzyme has a key role in maintaining metal homeostasis. Moreover, these phenomena appear as the predictable consequence of HMA2 driving the export of metals from the cytoplasm and being located in the plasma membrane rather than in an intracellular organelle. Supporting this rationale, it can be considered that, if HMA2 would transport extracellular ions into the cytoplasm, a different phenotype (reduced metal levels) would be observed. Moreover, our results correlate with the recent studies involving transgenic expression of *E. coli* ZntA in Arabidopsis (Lee et al., 2003). ZntA appears to be targeted to the plasma membrane of Arabidopsis protoplasts; consequently, constitutive expression of this Zn^{2+}-ATPase leads to the reduction of Zn^{2+} total levels in plants. However, in this analysis we should also consider the

phenotypes observed in *hma2*, *hma4*, and *hma2 hma4* double mutants (Hussain et al., 2004). It was reported that shoots from the *hma2-2* mutant (in the Wassilewskija ecotype background) had Zn^{2+} levels similar to wild-type plants when grown in agar in the absence or presence of 10 μM Zn^{2+}. Although the apparent lack of phenotype might be due to the different mutant or ecotype tested, we think that more likely the differences might be attributable to the distinct experimental conditions. In our studies, metal levels were measured in plants grown in soil, receiving an exposure to higher metal levels (0.5 mM Zn^{2+}). Hussain et al. (2004) also observed a decrease in Zn^{2+} levels after irrigating soil-grown *hma2 hma4* double mutants with water or 1 mM Zn^{2+}. In this case, it is likely that the effect of the *hma2* mutation was masked by the *hma4* knockout since this mutation seems to prevent translocation of Zn^{2+} from roots to shoots, thus leading to a decreased metal level (Hussain et al., 2004).

The analysis of HMA2 function should also consider the tissue distribution of this protein. The expression of a reporter gene under the control of the HMA2 promoter region shows that HMA2 is likely expressed in vascular tissues (Hussain et al., 2004). On the other hand, metal exposure seems to have little effect on HMA2 transcript expression. Thus, transcript levels and reporter gene location in conjunction with the plasma membrane location of the protein and the observed direction of transport suggest that HMA2 might have a central role in Zn^{2+} uploading into the vasculature, particularly the phloem, while HMA4 might have a more predominant role in xylem uploading in roots. Assuming that apoplastic metal levels influence the kinetics of the various metal transporters and thus the intracellular metal levels, it can be hypothesized that, indirectly, these two Zn-ATPases affect the overall Zn^{2+} homeostasis in plants by controlling the loading of this metal into the vasculature.

In summary, our results indicate that HMA2 is a Zn^{2+}-transporting ATPase that drives the efflux of the metal into the extracellular compartment. Consequently, *HMA2* gene knockouts lead to increased levels of Zn^{2+}. The enzyme has high metal affinity and broad specificity, thus also controlling levels of non-physiological heavy metals such as Cd^{2+}.

MATERIALS AND METHODS

Plant Growth

Arabidopsis (*Arabidopsis thaliana* ecotype Columbia) seeds were sterilized for 1 min in 70% (v/v) ethanol followed by soaking for 5 min in 1.25% (v/v) bleach solution supplemented with 0.02% Triton X-100. After incubation at 4°C for 48 h, seedlings were grown vertically on 2% agar, Murashige and Skoog salt-base medium (Buer et al., 2000). Wild-type seedlings were exposed to various metal stress conditions by growing them in Murashige and Skoog medium supplemented with one of the following metals (mM): $ZnSO_4$ (0.5); $CdCl_2$ (0.25); $CoCl_2$ (0.25); $CuSO_4$ (0.1); $AgNO_3$ (0.1); $MnCl_2$ (0.25); $NiSO_4$ (0.25). Arabidopsis Columbia plants were grown in soil in a plant growth chamber at 22°C, 10,000 to 14,000 lux cool-white fluorescent light intensity under a 14-h day/10-h night cycle. Soil-grown plants were exposed to Zn^{2+} and Cd^{2+} by drenching them in either 0.5 mM $ZnCl_2$ or 0.125 mM $CdCl_2$ solutions every 5 d.

HMA2 Cloning

First-strand *HMA2* cDNA was obtained from Arabidopsis leaf RNA by using SuperScript II reverse transcriptase (Invitrogen, Carlsbad, CA) and an oligo(dT) primer. Second-strand synthesis was done by PCR using the first-strand cDNAs as templates and forward and reverse primers corresponding to the 5′ and 3′ ends of the *HMA2* predicted coding sequence (forward, 5′-ATGGCGTCGAAGAAGATGACC-3′; reverse, 5′-TTCAATCACAATCTC-TTTCAAGGT-3′; At-genome, At4g30110; accession no. AY434728). Resulting cDNA was purified and ligated into the pBAD/TOPO vector (Invitrogen). The cDNA sequence was confirmed by automated DNA sequence analysis.

HMA2 Expression in Yeast

HMA2 cDNA was subcloned into the *Kpn*I and *Xho*I sites of the yeast (*Saccharomyces cerevisiae*) expression vector pYES2/CT (Invitrogen) under the control of a *GAL*-inducible promoter. This vector introduces a His_6 tag at the C-terminal end of the protein. In control experiments, an HMA2 stop codon was included in the insert. The resulting protein lacking the His_6 tag was used to verify that the tag did not alter measured kinetic parameters. The forward primer used for *HMA2* cDNA amplification was designed to include a yeast consensus sequence (AATA) upstream of the initiation codon, as suggested by the vector supplier. Yeast strain INVSc1 MATα *his3Δ1 leu2 trp1-289 ura3-52* (Invitrogen) was transformed with the HMA2-pYES2/CT or the empty pYES2/CT vector by the lithium acetate method (Ito et al., 1983), and uracil-based selection was used to screen for transformants. Yeast cells were grown overnight at 30°C in synthetic dextrose medium without uracil (6.7 g L^{-1}, yeast nitrogen base, 1.92 g L^{-1} yeast synthetic dropout media without uracil [Sigma, St. Louis]) supplemented with 20 g L^{-1} Glc. To induce HMA2 expression, cells were diluted to OD_{600} = 0.4 with the same media but containing 20 g L^{-1} Gal instead of Glc and grown for 8 h.

Yeast Membrane Preparation

Membrane preparation from yeast cells was done as previously described with minor modifications (Voskoboinik et al., 2001). Briefly, cells were suspended in 10 mM Tris (pH 7.4), 250 mM Suc, 10 mM ascorbic acid, 1 mM phenylmethylsulfonyl fluoride, 1 μg mL^{-1} leupeptin, and 1 μg mL^{-1} aprotinin. Cells were disrupted in a bead beater (BioSpec, Bartlesville, OK; 4 × 30 s homogenization with 30-s intervals) and the homogenate was centrifuged at 10,000*g* for 20 min. The supernatant was collected and centrifuged at 110,000*g* for 60 min. The resulting pellet was resuspended in the buffer described above except that it contained 0.2 mM ascorbic acid. All procedures were performed at 0°C to 4°C. The membrane preparations (7–10 mg protein mL^{-1}) were stored at −80°C. Protein was measured in accordance with Bradford (1976), using bovine serum albumin as a standard. SDS-PAGE was carried out in 10% acrylamide gels (Laemmli, 1970). Protein bands were observed by staining the gels with Coomassie Brilliant Blue. Heterologous protein was detected by electroblotting the gels onto nitrocellulose membranes and immunostaining with anti-His_6 rabbit polyclonal IgG (Santa Cruz Biotechnology, Santa Cruz, CA) and donkey anti-rabbit IgG-horseradish peroxidase-linked monoclonal antibody (Santa Cruz Biotechnology).

ATPase Assays

The ATPase assay mixture contained 50 mM Tris, pH 7.5, 3 mM $MgCl_2$, 3 mM ATP, 20 mM Cys, 1 mM dithiothreitol (DTT), 0.5 mg mL^{-1} saponin, 1 μM $ZnCl_2$ (or the metal indicated in the figures), and 40 μg mL^{-1} protein (membrane preparation). In different experiments, these reagents were independently varied as indicated in the corresponding figures. ATPase activity was measured for 15 min at 30°C. Released inorganic phosphate was colorimetrically determined (Lanzetta et al., 1979). Background activity measured in the absence of transition metals or in membranes from empty vector-transformed yeast was less than 20% to 30% of the Zn^{2+}- or Cd^{2+}-stimulated activity present in HMA2-containing membranes. This background was subtracted from the activity measured in the presence of metals.

Phosphorylation Assays

Enzyme phosphorylation by ATP was carried out at 0°C in a medium containing 50 mM Tris, pH 7.5, 0.5 mg mL^{-1} saponin, 1 mM $MgCl_2$, 5 μM [γ-^{32}P] ATP (MP Biomedical, Irvine, CA), 0.04 mM EGTA, 20 mM Cys, 20% dimethyl

sulfoxide, 100 μg mL^{-1} protein (membrane preparation), and 2.5 μM metal as indicated in Figure 6. Vanadate inhibition was measured by including 1.5 mM Na_3VO_4 in the assay medium. The reaction was initiated by the addition of [γ-^{32}P] ATP. After 1 min incubation, phosphorylation was stopped with five volumes of ice-cold 10% TCA and 1 mM inorganic phosphate. In initial experiments, samples were centrifuged at 14,000*g* for 10 min, resuspended in acidic SDS-PAGE loading buffer (5 mM Tris-PO_4, pH 5.8, 6.7 M urea, 0.4 M DTT, 5% SDS, and 0.014% bromphenol blue), and resolved by SDS-PAGE in 8% acidic gels (Sarkadi et al., 1986). The gels were dried and radioactivity was monitored in a phosphoimager. In subsequent experiments, the samples were filtered through nitrocellulose 0.45-μm filters (Millipore, Billerica, MA), washed five times with acid-stopping solution, and radioactivity was measured in a scintillation counter. Background phosphorylation measured in the absence of transition metals or in membranes from empty vector-transformed yeast was less than 5% to 10% of the Zn^{2+}- or Cd^{2+}-stimulated activity present in HMA2-containing membranes. This background was subtracted from phosphorylation measured in the presence of metals.

Zn^{2+} Transport Assays

The assay mixture contained 50 mM Tris, pH 7.5, 3 mM $MgCl_2$, 3 mM ATP, 5 mM Cys, 1 μM $ZnCl_2$, 5 μM FluoZin-1 (Molecular Probes, Eugene, OR), and 100 μg mL^{-1} protein (membrane preparation). Vanadate inhibition was tested by including 1.5 mM Na_3VO_4 in the assay medium. Metal uptake was initiated by the addition of ATP. Zn-FluoZin-1 was excited at 495 nm and emission measured at 520 nm. The indicator showed a linear fluorescent response in the 0.25- to 5-μM Zn^{2+} range. None of the reagents in the assay media produced detectable fluorescence quenching. Determinations were performed at 25°C.

mRNA Level Analysis

Total RNA was isolated using the RNeasy-Midi kit (Qiagen, Valencia, CA) from Arabidopsis 10-d-old seedlings grown either in agar plates containing Murashige and Skoog or Murashige and Skoog supplemented with various metals (see above) and from soil-grown 6-week-old plants (roots, leaves, stems, and flowers). cDNA synthesis was performed with SuperScript III reverse transcriptase (Invitrogen) and oligo(dT) as primer. The PCR amplification was performed with a cDNA aliquot and gene-specific primers for *HMA2* (forward, 5′-TGCTGTACATCGGAGGTTCCGT-3′ and reverse, 5′-CACTGAGCAACAACATGCTATTAAGG-3′) and the ubiquitous *eEF1α* (forward, 5′-AGGAGCCCAAGTTTTTGAAGA-3′ and reverse, 5′-TTCTTCACTGCAGCCTTGGT-3′). Samples were taken after each cycle and amplified bands quantified in agarose gels to verify that saturation has not been reached. Consistent results were obtained in two fully independent experiments.

Northern-Blot Analysis

Total RNA was extracted as indicated and denatured by incubating 15 min at 55°C. Samples were separated by denaturing agarose gel electrophoresis and transferred to Immobilon nylon membranes (Millipore; Sambrook et al., 1989). Equal loading of RNA in each lane was confirmed by ethidium bromide staining of 18S rRNA. Probes were prepared by amplification of a 1,420-bp DNA fragment that is complementary to the cDNA fragment between 49 and 1,469 bp. Probes were labeled with [α-^{32}P]dATP (Amersham Biosciences, Piscataway, NJ) by random hexamer primers. After hybridization at 65°C, the nylon membranes were washed twice for 15 min at 65°C in a low-stringency wash solution (2× SSC/0.1% SDS). Radiolabeled bands were detected by autoradiography.

Metal Content Analysis

Determinations were performed using whole-plant samples (approximately 250 mg) from 4-week-old wild-type and mutant plants. Three plants were pooled for each independent determination. Samples were washed with distilled water, drained, and acid digested at 80°C for 4 h and then overnight at room temperature with 7 mL 4.5 N HNO_3. After digestion, 0.5 mL 30% H_2O_2 were added and samples diluted with water to 10-mL final volume. Metal (Zn, Fe, and Cd) contents were measured by atomic absorption spectroscopy (AAnalyst 300; Perkin-Elmer, Foster City, CA).

Insertional Mutant Isolation

The Salk_034393 Arabidopsis line carrying a T-DNA insert approximately 140 bp from the start of the first intron in the *HMA2* gene (Alonso et al., 2003) was obtained from the Arabidopsis Biological Resource Center (ABRC). Homozygous mutants (referred to as *hma2-4* in this article) were identified by PCR screening using genomic DNA as template and separated combinations of a primer sitting in the left border of the T-DNA insert (5′-GCGTGGACCGCTTGCTGCAACT-3′; primer C in Fig. 9) and *HMA2*-specific primers (forward, 5′-CGACAACGTTATCATTCATACCCATC-3′ and reverse, 5′-AATTGGTTTCTCCGGTTACCCTCAC-3′; primers A and B, respectively, in Fig. 9). The absence of a full-length *HMA2* transcript was confirmed by RT-PCR (forward, 5′-TGCTGTACATCGGAGGTTCCGT-3′ and reverse, 5′-CACTGAGCAACAACATGCTATTAAGG-3′; primers D and E in Fig. 9) and northern-blot analysis. The *hma2-5* mutant was obtained from Jeffrey Harper's laboratory (The Scripps Research Institute, La Jolla, CA). This mutant is homozygous for a T-DNA insertion in the fourth exon of the *HMA2* gene (404_B12; Syngenta, San Diego). The absence of a full-length *HMA2* transcript in *hma2-5* mutant plants was confirmed by RT-PCR analysis in our laboratory.

Material Distribution

Upon request, all novel materials described in this publication will be made available in a timely manner for noncommercial research purposes subject to the requisite permission from any third-party owners of all or parts of the material. Obtaining any permissions will be the responsibility of the requester.

Sequence Analysis

Sequences were aligned using the LaserGene software package (DNASTAR, Madison, WI). HMA2 membrane topology was obtained using the TMHMM 2.0 on-line server for prediction of transmembrane helices (http://www.cbs.dtu.dk/services/TMHMM).

Data Analysis

Curves of ATPase activity versus metal were fit to $v = V_{max}\,L/(L + K_{1/2})$, where L is the concentration of variable ligand. ATPase activity versus vanadate curves were fit to $v = (V_{max} - V_{min})/[1 + (I/K_{1/2})] + V_{min}$, where I is the concentration of inhibitor, $K_{1/2}$ is the inhibitor concentration that produces one-half the inhibitory effect, and V_{min} is the activity at maximum inhibition. Data analysis was done using the KaleidaGraph software (Synergy, Reading, PA). The reported SEs for V_{max} and K_m are asymptotic SEs reported by the fitting program.

Sequence data from this article have been deposited with the EMBL/GenBank data libraries under accession number AY434728.

ACKNOWLEDGMENTS

We are grateful to Dr. Jeffrey F. Harper (The Scripps Research Institute, La Jolla, CA) for generously providing us with the homozygous *hma2-5* mutant line and Dr. Chris Cobbett (University of Melbourne, Victoria, Australia) for sending us an advance copy of his latest manuscript. We thank Dr. Craig Fairchild and Dr. Kristin Wobbe (Worcester Polytechnic Institute, Worcester, MA) for helpful discussions and advice. We also thank Don Pellegrino (Worcester Polytechnic Institute) for his assistance with metal content determinations.

Received May 28, 2004; returned for revision July 19, 2004; accepted July 23, 2004.

LITERATURE CITED

Alonso JM, Stepanova AN, Leisse TJ, Kim CJ, Chen H, Shinn P, Stevenson DK, Zimmerman J, Barajas P, Cheuk R, et al (2003) Genome-wide insertional mutagenesis of Arabidopsis thaliana. Science **301:** 653–657

Argüello JM (2003) Identification of ion selectivity determinants in heavy metal transport P1B-type ATPases. J Membr Biol **195:** 93–108

Axelsen KB, Palmgren MG (1998) Evolution of substrate specificities in the P-type ATPase superfamily. J Mol Evol **46:** 84–101

Axelsen KB, Palmgren MG (2001) Inventory of the superfamily of P-type ion pumps in Arabidopsis. Plant Physiol **126:** 696–706

Bateman A, Coin L, Durbin R, Finn RD, Hollich V, Griffiths-Jones S, Khanna A, Marshall M, Moxon S, Sonnhammer EL, et al (2004) The Pfam protein families database. Nucleic Acids Res **32:** D138–D141

Baxter I, Tchieu J, Sussman MR, Boutry M, Palmgren MG, Gribskov M, Harper JF, Axelsen KB (2003) Genomic comparison of p-type ATPase ion pumps in Arabidopsis and rice. Plant Physiol **132:** 618–628

Bradford MM (1976) A rapid and sensitive method for the quantitation of microgram quantities of protein utilizing the principle of protein-dye binding. Anal Biochem **72:** 248–254

Buer CS, Masle J, Wasteneys GO (2000) Growth conditions modulate root-wave phenotypes in Arabidopsis. Plant Cell Physiol **41:** 1164–1170

Bull PC, Cox DW (1994) Wilson disease and Menkes disease: new handles on heavy-metal transport. Trends Genet **10:** 246–252

Clemens S (2001) Molecular mechanisms of plant metal tolerance and homeostasis. Planta **212:** 475–486

Cobbett C, Goldsbrough P (2002) Phytochelatins and metallothioneins: roles in heavy metal detoxification and homeostasis. Annu Rev Plant Biol **53:** 159–182

Fan B, Rosen BP (2002) Biochemical characterization of CopA, the Escherichia coli Cu(I)- translocating P-type ATPase. J Biol Chem **277:** 46987–46992

Fraústro da Silva JJR, Williams RJP (2001) The Biological Chemistry of the Elements, Ed 2. Oxford Unviversity Press, New York

Gee KR, Zhou ZL, Ton-That D, Sensi SL, Weiss JH (2002) Measuring zinc in living cells. A new generation of sensitive and selective fluorescent probes. Cell Calcium **31:** 245–251

Gravot A, Lieutaud A, Verret F, Auroy P, Vavasseur A, Richaud P (2004) AtHMA3, a plant P1B-ATPase, functions as a Cd/Pb transporter in yeast. FEBS Lett **561:** 22–28

Guerinot ML (2000) The ZIP family of metal transporters. Biochim Biophys Acta **1465:** 190–198

Guerinot ML, Eide D (1999) Zeroing in on zinc uptake in yeast and plants. Curr Opin Plant Biol **2:** 244–249

Hacisalihoglu G, Hart JJ, Wang YH, Cakmak I, Kochian LV (2003) Zinc efficiency is correlated with enhanced expression and activity of zinc-requiring enzymes in wheat. Plant Physiol **131:** 595–602

Hall JL (2002) Cellular mechanisms for heavy metal detoxification and tolerance. J Exp Bot **53:** 1–11

Himelblau E, Mira H, Lin SJ, Culotta VC, Penarrubia L, Amasino RM (1998) Identification of a functional homolog of the yeast copper homeostasis gene ATX1 from Arabidopsis. Plant Physiol **117:** 1227–1234

Hirayama T, Kieber JJ, Hirayama N, Kogan M, Guzman P, Nourizadeh S, Alonso JM, Dailey WP, Dancis A, Ecker JR (1999) RESPONSIVE-TO-ANTAGONIST1, a Menkes/Wilson disease-related copper transporter, is required for ethylene signaling in Arabidopsis. Cell **97:** 383–393

Hou Z, Mitra B (2003) The metal specificity and selectivity of ZntA from Escherichia coli using the acylphosphate intermediate. J Biol Chem **278:** 28455–28461

Hussain D, Haydon MJ, Wang Y, Wong E, Sherson SM, Young J, Camakaris J, Harper JF, Cobbett CS (2004) P-type ATPase heavy metal transporters with roles in essential zinc homeostasis in Arabidopsis. Plant Cell **16:** 1327–1339

Ito H, Fukuda Y, Murata K, Kimura A (1983) Transformation of intact yeast cells treated with alkali cations. J Bacteriol **153:** 163–168

La Fontaine S, Firth SD, Lockhart PJ, Brooks H, Camakaris J, Mercer JF (1999) Functional analysis of the Menkes protein (MNK) expressed from a cDNA construct. Adv Exp Med Biol **448:** 67–82

Laemmli UK (1970) Cleavage of structural proteins during the assembly of the head of bacteriophage T4. Nature **227:** 680–685

Lanzetta PA, Alvarez LJ, Reinach PS, Candia OA (1979) An improved assay for nanomole amounts of inorganic phosphate. Anal Biochem **100:** 95–97

Lee J, Bae H, Jeong J, Lee JY, Yang YY, Hwang I, Martinoia E, Lee Y (2003) Functional expression of a bacterial heavy metal transporter in Arabidopsis enhances resistance to and decreases uptake of heavy metals. Plant Physiol **133:** 589–596

Lutsenko S, Kaplan JH (1995) Organization of P-type ATPases: significance of structural diversity. Biochemistry **34:** 15607–15613

Lutsenko S, Petris MJ (2003) Function and regulation of the mammalian copper-transporting ATPases: insights from biochemical and cell biological approaches. J Membr Biol **191:** 1–12

Mana-Capelli S, Mandal AK, Argüello JM (2003) Archaeoglobus fulgidus CopB is a thermophilic Cu^{2+} - ATPase. Functional role of its histidine-rich N-terminal metal binding domain. J Biol Chem **278:** 40534–40541

Mandal AK, Argüello JM (2003) Functional roles of metal binding domains of the Archaeoglobus fulgidus Cu^{+} ATPase CopA. Biochemistry **42:** 11040–11047

Mandal AK, Cheung WD, Argüello JM (2002) Characterization of a thermophilic P-type Ag^{+}/Cu^{+}-ATPase from the extremophile *Archaeoglobus fulgidus*. J Biol Chem **277:** 7201–7208

Marschner H (1995) Mineral Nutrition of Higher Plants, Ed 2. Academic Press, London

Maser P, Thomine S, Schroeder JI, Ward JM, Hirschi K, Sze H, Talke IN, Amtmann A, Maathuis FJ, Sanders D, et al (2001) Phylogenetic relationships within cation transporter families of Arabidopsis. Plant Physiol **126:** 1646–1667

Melchers K, Weitzenegger T, Buhmann A, Steinhilber W, Sachs G, Schofer KP (1996) Cloning and membrane topology of a P type ATPase from *Helicobacter pylori*. J Biol Chem **271:** 446–457

Mills RF, Krijger GC, Baccarini PJ, Hall JL, Williams LE (2003) Functional expression of AtHMA4, a P1B-type ATPase of the Zn/Co/Cd/Pb subclass. Plant J **35:** 164–176

Okkeri J, Haltia T (1999) Expression and mutagenesis of ZntA, a zinc-transporting P-type ATPase from *Escherichia coli*. Biochemistry **38:** 14109–14116

Outten CE, O'Halloran TV (2001) Femtomolar sensitivity of metalloregulatory proteins controlling zinc homeostasis. Science **292:** 2488–2492

Pedersen PL, Carafoli E (1987) Ion motive ATPases: I. Ubiquity, properties, and significance to cell function. Trends Biochem Sci **12:** 146–150

Rae TD, Schmidt PJ, Pufahl RA, Culotta VC, O'Halloran TV (1999) Undetectable intracellular free copper: the requirement of a copper chaperone for superoxide dismutase. Science **284:** 805–808

Rauser WE (1999) Structure and function of metal chelators produced by plants: the case for organic acids, amino acids, phytin, and metallothioneins. Cell Biochem Biophys **31:** 19–48

Rea PA (1999) MRP subfamily ABC transporters from plants and yeast. J Exp Bot **50:** 895–913

Rensing C, Ghosh M, Rosen BP (1999) Families of soft-metal-ion-transporting ATPases. J Bacteriol **181:** 5891–5897

Rensing C, Mitra B, Rosen BP (1998a) The zntA gene of *Escherichia coli* encodes a Zn(II)-translocating P-type ATPase. J Biol Chem **273:** 3765–3770

Rensing C, Mitra B, Rosen BP (1998b) A Zn(II)-translocating P-type ATPase from *Proteus mirabilis*. Biochem Cell Biol **76:** 787–790

Rutherford JC, Cavet JS, Robinson NJ (1999) Cobalt-dependent transcriptional switching by a dual-effector MerR-like protein regulates a cobalt-exporting variant CPx-type ATPase. J Biol Chem **274:** 25827–25832

Sambrook J, Fritsch EF, Maniatis T (1989) Molecular Cloning. A Laboratory Manual. Cold Spring Harbor Laboratory Press, Cold Spring Harbor, NY

Sarkadi B, Enyedi A, Foldes-Papp Z, Gardos G (1986) Molecular characterization of the in situ red cell membrane calcium pump by limited proteolysis. J Biol Chem **261:** 9552–9557

Sharma R, Rensing C, Rosen BP, Mitra B (2000) The ATP hydrolytic activity of purified ZntA, a Pb(II)/Cd(II)/Zn(II)-translocating ATPase from *Escherichia coli*. J Biol Chem **275:** 3873–3878

Shikanai T, Muller-Moule P, Munekage Y, Niyogi KK, Pilon M (2003) PAA1, a P-type ATPase of Arabidopsis, functions in copper transport in chloroplasts. Plant Cell **15:** 1333–1346

Solioz M, Odermatt A (1995) Copper and silver transport by CopB-ATPase in membrane vesicles of *Enterococcus hirae*. J Biol Chem **270:** 9217–9221

Solioz M, Vulpe C (1996) CPx-type ATPases: a class of P-type ATPases that pump heavy metals. Trends Biochem Sci **21:** 237–241

Tsai KJ, Lin YF, Wong MD, Yang HH, Fu HL, Rosen BP (2002) Membrane topology of the p1258 CadA Cd(II)/Pb(II)/Zn(II)-translocating P-type ATPase. J Bioenerg Biomembr **34:** 147–156

Tsai KJ, Linet AL (1993) Formation of a phosphorylated enzyme intermediate by the cadA Cd(2+)-ATPase. Arch Biochem Biophys **305:** 267–270

Tsai KJ, Yoon KP, Lynn AR (1992) ATP-dependent cadmium transport by

the cadA cadmium resistance determinant in everted membrane vesicles of *Bacillus subtilis*. J Bacteriol **174:** 116–121

Voskoboinik I, Brooks H, Smith S, Shen P, Camakaris J (1998) ATP-dependent copper transport by the Menkes protein in membrane vesicles isolated from cultured Chinese hamster ovary cells. FEBS Lett **435:** 178–182

Voskoboinik I, Mar J, Strausak D, Camakaris J (2001) The regulation of catalytic activity of the Menkes copper-translocating P-type ATPase. Role of high affinity copper-binding sites. J Biol Chem **276:** 28620–28627

Voskoboinik I, Strausak D, Greenough M, Brooks H, Petris M, Smith S, Mercer JF, Camakaris J (1999) Functional analysis of the N-terminal CXXC metal-binding motifs in the human Menkes copper-transporting P-type ATPase expressed in cultured mammalian cells. J Biol Chem **274:** 22008–22012

Williams LE, Pittman JK, Hall JL (2000) Emerging mechanisms for heavy metal transport in plants. Biochim Biophys Acta **1465:** 104–126

Woeste KE, Kieber JJ (2000) A strong loss-of-function mutation in RAN1 results in constitutive activation of the ethylene response pathway as well as a rosette-lethal phenotype. Plant Cell **12:** 443–455

Woolhouse HW (1983) Toxicity and tolerance in the responses of plants to metals. *In* OL Lange, PS Nobel, CB Osmond, H Ziegler, eds, Physiological Plant Ecology III. Responses to the Chemical and Biological Environment, Vol 12C. Springer-Verlag, Berlin